Measurement of the $^{25}Al(d,n)^{26}Si$ reaction and impact on the $^{25}Al(p,\gamma)^{26}Si$ reaction rate

E. Temanson, J. Baker, K. Hanselman, G. W. McCann, L. T. Baby, A. Volya, P. Höflich, and I. Wiedenhöver Department of Physics, Florida State University, Tallahassee, Florida 32306, USA (Dated: May 22, 2023)

The $^{25}{\rm Al}({\rm p},\gamma)^{26}{\rm Si}$ reaction is part of a reaction network with impact on the observed galactic $^{26}{\rm Al}$ abundance. A new determination of the proton strength of the lowest $\ell=0$ proton-resonance in $^{26}{\rm Si}$ is required to more precisely calculate the thermal reaction rate. To this end, the $^{25}{\rm Al}({\rm d},{\rm n})^{26}{\rm Si}$ proton-transfer reaction is measured in inverse kinematics using an in-flight radioactive beam at the RESOLUT facility. Excitation energies of the lowest $^{26}{\rm Si}$ proton resonances are measured and cross sections are determined for the lowest $\ell=0$ resonance associated with the 3_3^+ state at 5.92(2) MeV. Coupled reaction channels (CRC) calculations using FRESCO are performed to extract the $\ell=0$ spectroscopic factor for the 3_3^+ state. The proton width for the 3_3^+ state in $^{26}{\rm Si}$ is determined to be $\Gamma_p{=}2.19(45)$ eV and the (p,γ) resonance strength for the 3_3^+ state is extracted as 26(10) meV. This resonance dominates the $^{25}{\rm Al}({\rm p},\gamma)^{26}{\rm Si}$ reaction rate above 0.2 GK.

I. INTRODUCTION

The observation of the 1.809 MeV γ -ray associated with the radioactive decay of 26 Al in 1982 by HEA0-3 marked the first experimental evidence of ongoing nucleosynthesis in the galaxy [1]. Further improvements in γ -ray astronomy have allowed telescopes such as COMPTEL [2] and INTEGRAL [3] to probe the spatial emission of the 1.809 MeV γ -ray across the galactic plane. Based on the emissions along the plane of the galaxy and an increased intensity near known massive star groups, the likely production cites for 26 Al are core-collapse supernova and Wolf-Rayet stars [4].

The presence of a low-lying isomeric 0^+ state, $^{26}Al^m$, whose population can only slowly reach thermal equilibrium with the 5⁺ ²⁶Al^g ground state, severely complicates the calibration of its nucleosynthesis. In discussions of the subject, beginning with Ref. [5] it is found that thermal equilibrium between $^{26}\mathrm{Al}^g$ and $^{26}\mathrm{Al}^m$ will typically be reached at temperatures above 0.4 GK, where indirect γ -absorption and emission competes with the $T_{1/2} = 6.345s \ \beta^+$ -decay of $^{26}\text{Al}^m$. Since this super-allowed β^+ -decay exclusively populates the ²⁶Mg ground state, it is in effect bypassing the 1.808 MeV γ -ray, on which the γ -ray astronomical observation is based. In consequence, the nucleosynthesis yield of ²⁶Al^g depends on the nuclear reactions leading to both ²⁶Al^g and ²⁶Al^m, their destruction rates, and the rates of equilibration processes between them. Both the ground and isomeric states are produced by the reaction $^{25}\mathrm{Mg}(\mathrm{p},\gamma)^{26}\mathrm{Alg,m}$. However, at sufficiently high temperatures, the $^{24}{\rm Mg}(p,\gamma)^{25}{\rm Al}$ reaction followed by the $^{25}{\rm Al}(p,\gamma)^{26}{\rm Si}$ reaction becomes competitive to produce 26 Si, which then decays exclusively to 26 Al m .

Motivated by the implications on γ -ray astronomy, multiple works have addressed the spectrum of proton resonances in $^{26}\mathrm{Si}$ and their relative impact on the $^{25}\mathrm{Al}(\mathrm{p},\gamma)$ reaction. Several experiments used indirect methods, through the $^{28}\mathrm{Si}(\mathrm{p,t})$ [6, 7], the $^{24}\mathrm{Mg}(^{3}\mathrm{He},n)$ [8] and the $^{29}\mathrm{Si}(^{3}\mathrm{He},^{6}\mathrm{He})$ [9] reactions. Other works used

 γ –spectroscopy after the (³He,n) reaction, [10, 11] to establish some level energies with high accuracy. A comprehensive analysis of the resonance spectrum by Chipps et al. [12] combined the available information from multiple works and, in particular, identified the dominant $\ell=0$ resonance with the 3_3^+ state at 5.9276(10) MeV of excitation energy. In the following, we will use the excitation energy from the NNDC data base [13], 5.9294(8) MeV and the corresponding center-of-mass resonance energy 0.4154(8) MeV.

Information on the strength of the 26 Si resonances in question was also obtained in studies investigated the isospin-mirror nucleus 26 Mg via the 25 Mg(d,p) 26 Mg reaction [14–16]. The most recent study of 26 Mg by C. B. Hamill et~al. [14] focused on the important 3^+ and 0^+ analog states at 6.125 and 6.255 MeV respectively and reported an upper limit for the lowest 1^+ state at 5.69 MeV.

As a first radioactive-beam experiment at FSU's RES-OLUT facility [17], Peplowski et al. [18] measured the proton-spectra following the ²⁵Al(d, n)²⁶Si transfer reaction in inverse kinematics and extracted the proton width of 19–52 meV for 0.4154(8) MeV resonance. Subsequently Bennett et al. [19] and Liang et al. [20] used the β^+ -decay of ²⁶P to populate the resonance spectrum in 26 Si and to determine the γ -proton branching ratio of the 0.4154(8) MeV resonance. With the same goal, Perello et al. [11] populated the resonances through the 24 Mg(3 He,n) 26 Si reaction and performed neutron- γ coincidence spectroscopy, obtaining results consistent with [19] and [20]. Those works determined the partial γ width of the 0.4154(8) MeV resonance by combining their respective γ -proton branching ratios with the partial proton width extracted by Peplowski et al. [18].

The present work describes a re-measurement of the 25 Al(d, n) 26 Si transfer reaction to determine the $\ell=0$ proton-strength of the 3_3^+ resonant state with improved methods and higher precision than Peplowski *et al.* [18].

II. THE ²⁵Al(d, n)²⁶Si EXPERIMENT

The experiment used a beam of the radionuclide ²⁵Al. produced with the RESOLUT facility [17] at the John D. Fox accelerator laboratory of Florida State University. The beam of $^{25}\mathrm{Al}$ was produced by bombarding a gas-cell target filled with D₂ gas, cooled to liquid-nitrogen temperatures, with the primary beam of ²⁴Mg, accelerated by the Tandem and superconducting LINAC facility to 142 MeV. The reaction products from the ²⁴Mg(d, n)²⁵Al reaction were separated and focused onto a secondary target through the RESOLUT facility, using a superconducting resonator to actively sharpen the particle energies and a magnetic spectrometer to separate the desired reaction products from the primary beam. A description of the principle of operation, the beam optics and a list of radioactive beams used in experiments is given in [17]. The optimal beam intensity was obtained at a magnetic rigidity of 0.5597 Tm, corresponding to 102 MeV of ²⁵Al in the 13^+ charge state.

The beam intensity and purity were monitored continuously in a zero-degree ion chamber, which is part of the experimental setup described below. The beam components were identified and separated by their characteristic energy losses, as displayed in Fig. 1, where the $^{25}{\rm Al}$ particles were well-separated from the $^{24}{\rm Mg}$ beam background. The secondary beam of interest, $^{25}{\rm Al}$, had an average beam intensity of 7.5×10^3 particles per second, which corresponded to a beam purity of 25%. The $^{25}{\rm Al}$ beam particles were also identified and and selected during the event analysis through their characteristic time-correlation with the accelerator RF reference.

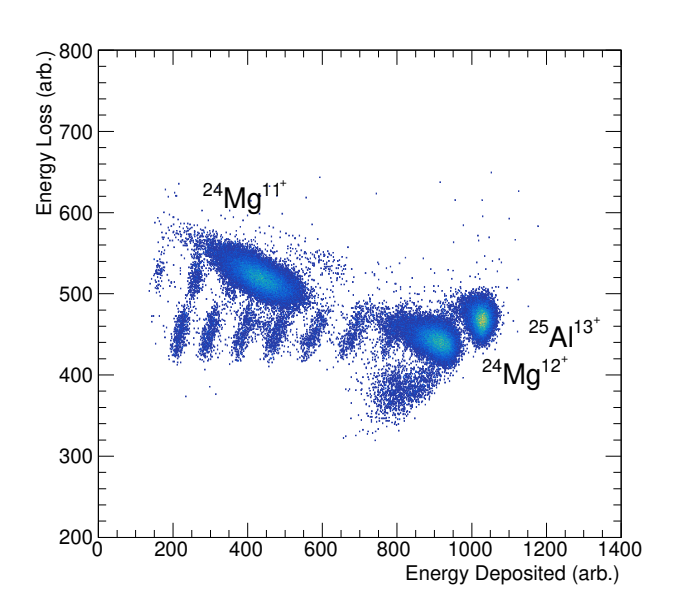


FIG. 1. Secondary beam composition measured in the gas ionization chamber.

The secondary beam of 25 Al bombarded a 512 $\mu g/cm^2$ thick deuterated polyethylene (CD_2) film. For detection of the decay protons, two annular Micron Semiconductor S2-type detectors with 64 μm and 1000 μm thicknesses were positioned at 69 mm and 82 mm downstream of the target, subtending angles between 8° and 22° from the beam axis. Each annular double-sided strip detector was read out in 16×16 channels, allowing for extraction of θ and ϕ for each particle. Signals from the beam particles and reaction residues were detected in a position-sensitive ion-chamber filled with 35 Torr of Isobutane gas. The ion chamber, see Ref. [21], was segmented into four depth regions. The first two sections of 40 mm depth allowed for a position-determination of the incoming particle in horizontal and vertical directions, the third and fourth section of 80 mm and 200 mm depth were used to determine the differential energy-loss and residual energy signals.

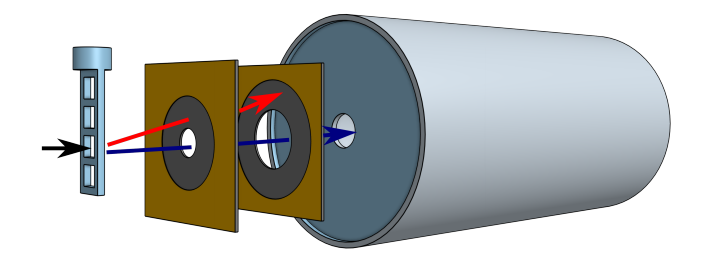


FIG. 2. Schematic representation of the experimental setup including the target ladder, silicon telescope and position sensitive ion chamber.

As the main trigger condition, events in either of the silicon detectors were recorded, along with the signals from the heavy-ion reaction residues and the timing information relative to the accelerator RF reference. In addition to the silicon-triggered events, the beam composition was continuously sampled by recording one of every 1000 events triggering the ion chamber. The silicon detectors were energy calibrated using standard calibration sources. The ion chamber sections were calibrated by matching the signals of the beam-components, whose energy was determined by the rigidity-measurement of RESOLUT, to a calculation of the deposited energies with the program CATIMA [22].

A. Experiment analysis

The excitation energy of 26 Si was reconstructed through the 26 Si* \rightarrow 25 Al+p decay path where both particles were detected in coincidence. The protons and 25 Al output channels were identified using their characteristic energy-loss vs. energy correlations observed in the silicon and ion-chamber detectors, respectively. Additional gates on the coincidence timing and a geometric correlation between both DSSD silicon detectors are applied.

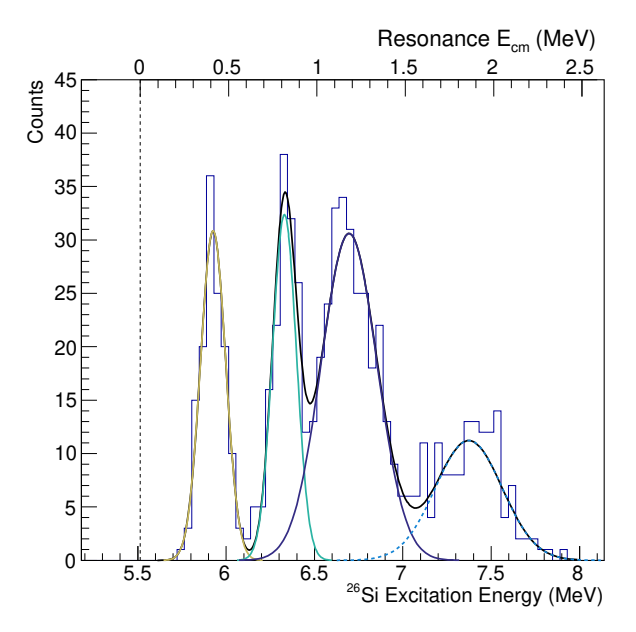


FIG. 3. Excitation energy spectrum of $^{26}\mathrm{Si}$. The secondary x-axis represents the associated center-of-mass proton resonance energies. The state of interest for astrophysical environments is the 3_3^+ at 5.92 MeV.

From the energies and emission directions of the coincident proton and $^{25}{\rm Al}$ particles the excitation energy of $^{26}{\rm Si}$ states was reconstructed through an invariant mass analysis. The resulting spectrum is displayed in Fig. 3, showing a strong peak at 5.92 MeV, a second peak at 6.33 MeV, a wider structure at 6.70 MeV and higher excited states near 7.40 MeV. The 5.92 MeV peak is identified with the 5.9294(8) MeV 3_3^+ state [13], at a resonance energy of 0.4154(8) MeV, the highest-impact resonance for the $^{25}{\rm Al}({\rm p},\gamma)^{26}{\rm Si}$ reaction.

A Monte-Carlo simulation was used to determine the coincident-detection efficiency of protons and reaction residues. The kinematics of the (d, n) neutrons and the subsequent proton decays were simulated in correlation, where the neutron angular distribution was weighted with a typical c.m. angular distribution, while all c.m.-proton angles entered evenly.

TABLE I. 26 Si excited states observed in 26 Si through the 25 Al(d,n) 26 Si reaction, with the corresponding cross sections.

E_x (MeV)	Adopted E_x^a (MeV)	$E_R^{c.m. a}$ (MeV)	J^{π}	$\sigma^{stat.}_{syst.}$ (mb)
5.92(2)	5.9294(8)	0.4154(8)	3_{3}^{+}	$5.83^{\pm 0.09}_{\pm 0.78}$
6.33(2)	$6.2953(24) \\ 6.3827(29)$	$0.7813(24) \\ 0.8687(29)$	2_{6}^{+} 2_{7}^{+}	$10.02^{\pm 0.09}_{\pm 1.42}$
6.70(2)	6.787(4)	1.273(4)	3_{1}^{-}	$30.12^{\pm 0.06}_{\pm 4.26}$

^a Nuclear data reference [13, 23]

The cross sections listed in Table I were extracted from the peak areas in the spectrum, the integrated number of beam particles determined from the ion chamber data, the target density and the simulated detection efficiency for the respective excitation energy. Here, the resonances are assumed to decay exclusively by proton emission. The uncertainties in the cross sections are largely from systematic uncertainties in the efficiency calculations and target thickness.

The measured cross section of the 3^+ state agrees with the previous measurement by Peplowski *et al.* [18], 8.7 ± 3 mbarn, with improved statistics and smaller uncertainty. Two additional peaks at 6.3 MeV and 6.7 MeV were measured as well. Peak 2 in Fig. 3 is comprised of two states with a combined cross section of 10(2) mb. Peak 3, observed with a total cross section of 30(4) mb, is likely associated with the 6.787 MeV 3_1^- state, but it is unclear if there is any contribution from additional states such as 6.76 or 6.81 MeV reported in Ref. [13].

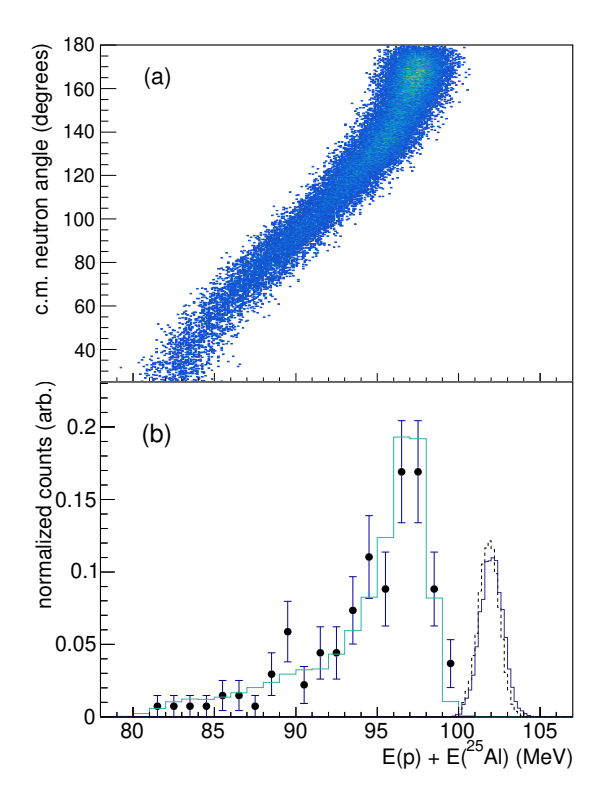


FIG. 4. (Panel a) Correlation between the $^{25}\mathrm{Al}+\mathrm{p}$ sum-energy and neutron-emission angle extracted from the Monte-Carlo simulation based on the (d,n) angular distribution from CRC theory (see text). (Panel b) The 5.92 MeV 3_3^+ experimental $^{25}\mathrm{Al}+\mathrm{p}$ sum-energy distribution compared to the results of the Monte-Carlo simulation. Shown for comparison is the experimental and simulated $^{25}\mathrm{Al}$ beam energy profile.

While the neutrons emitted in the (d,n) reaction remain undetected in the current experiment, the neutron energies leave an imprint as "missing" energy in the total energy of the ²⁶Si compound nucleus, which is recon-

structed from the proton and $^{25}\mathrm{Al}$ final-state particles. In Panel(a) of Fig. 4, the simulated correlation between the neutron angle in the center-of-mass system and the finalstate ²⁵Al+p sum-energy is displayed, based on calculated neutron angular distribution from the CRC model for this reaction, which itself will be described in the following section. Because of the strong kinematic variation of the (d,n) neutron energy with the emission angle, the energy distribution also contains information on the angular distribution. The distribution of the experimental ²⁵Al+p sum-energies for the 5.92 MeV 3⁺ state is displayed in Panel(b) of Fig. 4. The simulated energy spectrum shows an excellent fit to the data and the quality of agreement argues for the applicability of the CRC reaction model in the experimental analysis. A similar analysis has also been described and applied in Ref. [24].

B. Discussion of a potential ²⁶Si state at 5.95 MeV.

A recent paper by Canete et al. [25] described a 1⁻ state in ²⁶Mg located at 5.710 MeV, which was assigned as a mirror-state to a potential 5.95 MeV state in ²⁶Si, creating a large uncertainty in the nucleosynthesis calculations. This state had been observed by Caggiano et al. [9] through a (³He,⁶He) reaction at a magnetic spectrograph and subsequently confirmed by Parpottas et al. [8] in a (³He,n) reaction, which was analyzed through neutron time-of-flight spectroscopy. Applying the parameters suggested by Canete et al., the single-proton strength of this resonance would be small and below the sensitivity of our experiment.

However, we observe that the evidence for the existence of a resonance at this energy is weak: The 24 Mg(3 He, $n\gamma$) 26 Si reaction measured by Perello *et al.* [11] was performed with the same reaction at the same energy as Parpottas et al. and observed two resonances at 0.375(2) MeV (0^+) and 0.4138(11) MeV (3^+) , consistent with the number of peaks observed by Parpottas et al., but at slightly lower excitation energies. It can therefore be assumed that the energy calibration of Parpottas et al. was slightly wrong. The Caggiano et al. experiment is now the only information pointing to an additional state at this energy and has not been independently verified. It seems unlikely that such a 1⁻ state would not have been observed by Perello et al. through its dominant γ -decay. We conclude that there is insufficient evidence for this 1⁻ resonance in ²⁶Si and therefore do not include in the following analysis.

C. 3⁺₃ Resonance Parameters

The main goal in the analysis is the determination of the resonance proton-width for the 3^+ resonance, which is closely related to its $\ell=0$ spectroscopic factor. This experiment determined the total cross section for the population of this state in the (d,n) reaction, but the

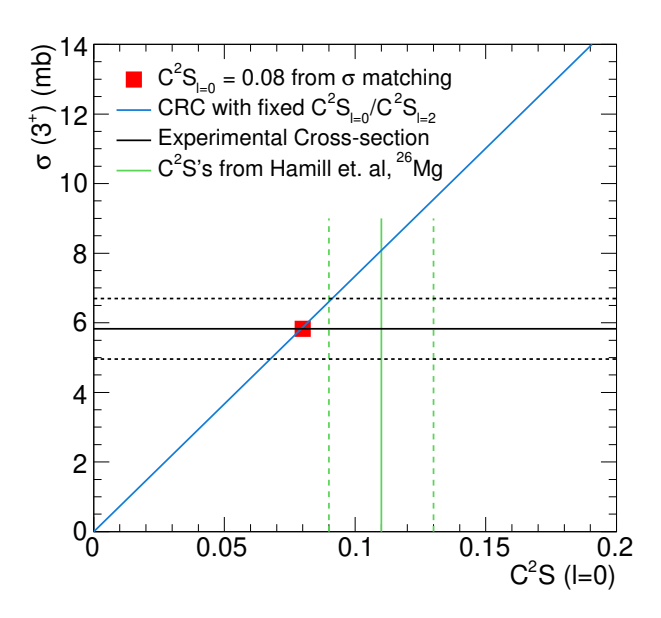


FIG. 5. Reaction cross sections from the CRC calculation (see text) in relation to the $C^2S_{l=0}$ spectroscopic factor. The values and error limits for the experimental cross section and the mirror-nucleus spectroscopic factors by Hamill $et\ al.\ [14]$ are marked. The blue line represents the cross section calculated while scaling the $C^2S_{l=0}$ and $C^2S_{l=2}$ proportionally.

limited experimental sensitivity to the neutron-angular distribution does not allow for the disentanglement of the $\ell=0$ and $\ell=2$ contributions. Here, we are relying on the mirror-reaction to guide the extraction of the relative $\ell=0$ component.

The reaction mechanism was investigated using a coupled reaction channels (CRC) calculation using the program FRESCO [26]. The entrance channel utilized the global deuteron optical model potentials from Haixia An and Chonghai Cai [27]. The exit channel was calculated using the global optical model parameters from A.J. Koning and J.P. Delarouche [28] assuming a neutron energy of 300 keV. The final states of interest in ²⁶Si are protonunbound and were calculated using a weak-binding approximation of 50 keV, which is justified through the relatively small widths of the states in question.

In Fig. 5 the method for extraction of the $\ell=0$ spectroscopic factor for the 3^+ resonance is illustrated. The experimental cross section and error interval are marked on the vertical axis. The spectroscopic factors determined in the mirror nucleus 26 Mg by Hamill et~al. [14] and the corresponding CRC cross section are also shown. Applying the mirror-nucleus spectroscopic factors directly would predict a slightly higher cross section than measured. Scaling the spectroscopic factors of Hamill et~al. down to reproduce the observed cross section arrives at an $\ell=0$ spectroscopic factor is $C^2S_{l=0}=0.079(16)$.

In order to extract the proton-resonance width from the $\ell=0$ spectroscopic factor, we employed the R-matrix expression

$$\Gamma_p = C^2 S_{l=0} \ \Gamma_{s.p.} = C^2 S_{l=0} \ \frac{\hbar^2 P_c}{\mu \ r_c} u^2(r_c),$$
 (1)

where r_c is the channel (interaction) radius, mu is the reduced mass, P_c is the penetrability of the Coulomb and centrifugal barriers and $u(r_c)$ is the radial wave function, which was extracted from the CRC calculation, evaluated at the channel radius $r_c = r_0(A^{1/3}+1)$ with $r_0 = 1.25$. At the adopted resonance energy, the proton single-particle width was calculated at the experimental resonance energy, resulting in $\Gamma_{s.p.} = 27.6(14)$ eV.

ergy, resulting in $\Gamma_{s.p.}=27.6(14)$ eV. The extracted $C^2S_{l=0}$ was multiplied with the proton single-particle width to extract $\Gamma_p=2.19(45)$ eV for the 3^+ resonance, which is in agreement with the previous value extracted by Peplowski *et al.*, within error limits [18]. The error associated with Γ_p is largely due to the systematic uncertainty in determining the $\ell=0$ spectroscopic factor, both the statistical and systematic uncertainty are reported in Table II.

III. THERMAL REACTION RATES

Reported in Table II are the relevant proton resonance parameters in $^{26}\mathrm{Si.}$ Included alongside this work's updated 3_3^+ parameters are the adopted 1_1^+ and 0_4^+ parameters from the $^{25}\mathrm{Mg}(\mathrm{d,p})^{26}\mathrm{Mg}$ reaction by Hamill et~al. [14] and the $^{24}\mathrm{Mg}(^3\mathrm{He,n})^{26}\mathrm{Si}$ reaction by Perello et~al. [11]. The Maxwell-averaged two-body reaction rate was calculated using the Breit-Wigner approximation for narrow resonances

$$N_A \langle \sigma \nu \rangle_r = \frac{1.5399 \times 10^{11}}{(\mu T_9)^{3/2}} \sum_i (\omega \gamma)_i e^{-11.605 E_{Ri}^{c.m.}/T_9}, (2)$$

where μ is the reduced atomic mass in a.m.u. from the AME 2020 compilation [23], $\mathbf{E}_{Ri}^{c.m.}$ is the center of mass resonance energy in MeV, T_9 is the temperature in units of GK. The resonance strength, $(\omega \gamma)$, is defined as

$$\omega \gamma = \frac{2J_r + 1}{(2J_p + 1)(2J_T + 1)} \left(\frac{\Gamma_p \Gamma_\gamma}{\Gamma_p + \Gamma_\gamma}\right), \quad (3)$$

where the spin of the proton is $J_p=1/2$, the spin of the 25 Al ground state is $J_T=5/2$ and J_r is the spin of the resonance. The proton partial width derived in this work is $\Gamma_p{=}2.19(45)$ for the 3_3^+ state, as discussed in Sec. II C. Because the 3^+ resonance decays predominantly by proton emission, the partial γ -width becomes the determining factor of the resonance strength $\omega\gamma$. However, this partial γ -width can be determined now with higher precision using the γ -proton branching ratios determined by other recent experiments [11, 19, 20]. A summary of the previous results is represented in Table II.

An interesting difference between the results obtained by Bennett et al. [19] and Liang et al. [20] lies in the respective normalization of the observed β^+ -delayed γ -decays relative to the β^+ -delayed proton decays. Bennett et al. only measured the β -delayed γ -decay intensity from the 3_3^+ state and normalized it relative to the β -delayed proton emission intensity from Thomas et al. [32]. In contrast, Liang et al. measured both branches in a single experiment. The proton-decay strength of 17.96(90) % from Thomas et al. [32] also appears problematic, since their values are inconsistent with the subsequent experiments by Liang et al. (11.1(12) %) [20] and Janiak et al.'s (10.4(9)-13.8(10) %) [31], which are consistent with each other.

It should be noted that the β^- -delayed γ -ray intensity for the 1742 keV $3_3^+ \to 3_2^+$ transition measured by Liang et~al.~[20] had significant statistical uncertainty and the authors used an error-weighted mean combining their results, Bennett et~al.~[19] and Pérez-Loureiro et~al.~[30], then calculating the proton-branching ratio from the Liang et~al.~ proton-decay probability.

The resonance parameters for the 1_1^+ and 0_4^+ states were adopted from the isospin-mirror reaction performed by Hamill *et al.* [14], the shell model calculations by Richter *et al.* [29] and the 24 Mg(3 He, $n\gamma$) 26 Si reaction by Perello *et al.* [11]. A 30% error was assumed for the resonance strength of these two states in the calculation of the reaction rate uncertainties.

The direct-capture component of the reaction rate is approximated using

$$\begin{split} N_A \langle \sigma \nu \rangle_{dc} &= 7.8327 \times 10^9 \left(S_{eff} \right) \left(\frac{Z_T}{\mu T_9^2} \right)^{1/3} \\ &\times \exp \left(-4.2487 \left(\frac{Z_T^2 \mu}{T_9} \right)^{1/3} \right) \quad (4) \end{split}$$

and

$$S_{eff} \approx S(0) \left(1 + 0.09807 \left(\frac{T_9}{Z_9^2 \mu} \right)^{1/3} \right),$$
 (5)

where Z_T is the atomic number of 25 Al and S_{eff} is the effective astrophysical S-factor. The zero energy point of the S-factor, S(0), which is dominated by the effects of direct proton capture, was adopted from Matic *et al.* [7] and the value 0.028 MeV-b, with an estimated 30% uncertainty.

In Fig. 6 each contribution to the reaction rate is plotted for temperatures up to 0.6 GK. As expected, above 0.2 GK, the 3_3^+ state dominates the total rate. The effect of the updated resonance parameters are shown in Fig. 7 where the rate from this work is compared to previously determined rates reported in the REACLIB database [33].

TABLE II. Parameters of the most important proton resonances in ²⁶ Si	with reference sources.	The values of the underlined
references were used in the reaction rate calculations (See Fig. 6 and Fig.		

J^{π}	Reference	$\mathbf{E}_{R}^{c.m.}$ (MeV)	C^2S	Γ_p (eV)	$\Gamma_{\gamma}/\Gamma_{p}$	$\Gamma_{\gamma} \text{ (eV)}$	$\omega \gamma \text{ (meV)}$
1_{1}^{+}	<u>Hamill et al.</u> [14]	$0.1622(3)^{a}$	$< 5.70 \times 10^{-3}$	$< 8.90 \times 10^{-9}$		$0.12^{\rm b}$	$< 2.60 \times 10^{-6}$
0_{4}^{+}	Hamill et al. [14]	$0.3761(3)^{a}$	0.042(10)	0.0042		$0.0088^{\rm b}$	0.24
0_{4}^{+}	Perello et al. [11]	0.375(2)		0.0042		$0.0075^{\rm c}$	0.22
3+	Bennett et al. [19]	0.4149(15)		$2.9(10)^{d}$	0.014(9) ^e	0.040(30)	23(17)
3_{3}^{+}	Hamill et al. [14]	$0.4154(8)^{a}$	0.11(2), 0.27(6)	$2.9(10)^{d}$	0.014(9)	$0.040^{\rm g}$	$23^{\rm g}$
3_{3}^{+}	Liang $et \ al. \ [20]$	$0.4124(19)^{\mathrm{f}}$		$2.9(10)^{\rm d}$	0.0207(75)	0.060(30)	34(17)
3_{3}^{+}	Perello et al. [11]	0.4138(11)		$2.9(10)^{d}$	0.025(14)	0.071(32)	40(17)
3_3^+	This work	$0.4154(8)^{a}$	0.079(16), 0.20(4)	$2.19 {}^{\pm 0.036}_{\pm 0.415} {}^{stat.}_{syst.}$	$0.021(8)^{lit.}$	0.045(17)	26(10)

^a Nuclear data references [13, 23]

f Error-weighted mean value from [20, 31, 32]

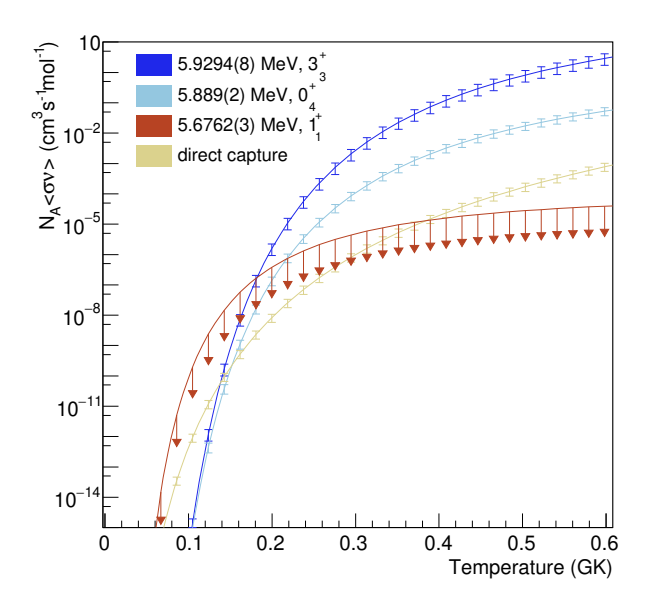


FIG. 6. Thermal rate for the $^{25}{\rm Al}({\rm p},\gamma)^{26}{\rm Si}$ reaction. The total rate is separated into direct capture (gold) and three individual resonance contributions, 1_1^+ (red), 0_4^+ (light blue) and 3_3^+ (dark blue).

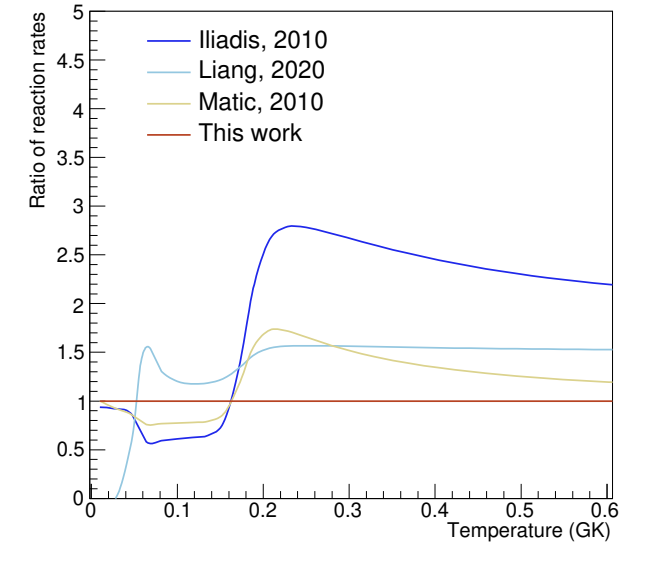


FIG. 7. Ratio of reaction rate from different rates reported in JINA's REACLIB database [33], compared to the current work.

IV. CONCLUSION

The proton decay from the 25 Al(d, n) 26 Si reaction was measured and the total cross section was obtained for the important 3_3^+ state at 5.92 MeV with higher precision and improved statistics than previously measured by Peplowski *et al.* [18]. A CRC calculation, using FRESCO [26], was used to extract spectroscopic information of the low-

est $\ell=0$ proton resonance, taking into account additional information obtained from the isospin mirror nucleus 26 Mg. An updated proton width, $\Gamma_p=2.19(45)$ eV, for the 3_3^+ state in 26 Si was extracted using the adopted resonance energy 0.4154(8) MeV and the branching ratio from Liang et al. [20]. The resulting resonance strength, 26(10) meV, was used to calculated the total reaction rate. Due to the decreased resonance strength of the 3_3^+ state, this work suggests a reduction in the reaction rate at temperatures above 0.2 GK.

^b Shell model calculation by Richter et al. [29]

^c Updated Richter et al.'s [29] result using new location of the 0⁺₄

^d Adopted from Peplowski *et al.* [18]

^e A complimentary reanalysis by Pérez-Loureiro et al. [30] reported $\Gamma_{\gamma}/\Gamma_{p}=0.015(5)$

g No uncertainties were provided in this reference.

ACKNOWLEDGMENTS

This work is partially supported by the National Science Foundation, under Award Number PHY-2012522. This material is partially based upon work supported by

the Department of Energy, National Nuclear Security Administration, under Award Number DE-NA0003841. The authors acknowledge the support of D. Caussyn, P.A. Barber, B. Schmidt and D. Spingler at the John D. Fox Accelerator Laboratory at Florida State University.

- W. Mahoney, J. Ling, A. Jacobson, and R. Lingenfelter, The Astrophysical Journal 262, 742 (1982).
- [2] R. Diehl, H. Steinle, A. Strong, V. Schoenfelder, M. Varendorff, K. Bennett, G. Lichti, H. Blömen, C. Dupraz, W. Hermsen, et al., COMPTEL observations of galactic ²⁶Al emission, Tech. Rep. (SCAN-9503047, 1994).
- [3] L. Bouchet, E. Jourdain, and J.-P. Roques, The Astrophysical Journal 801, 142 (2015).
- [4] R. Diehl, M. G. Krause, K. Kretschmer, M. Lang, M. M. Pleintinger, T. Siegert, W. Wang, L. Bouchet, and P. Martin, New Astronomy Reviews 92, 101608 (2021).
- [5] R. A. Ward and W. A. Fowler, Astrophys. J. 238, 266 (1980).
- [6] D. W. Bardayan, J. A. Howard, J. C. Blackmon, C. R. Brune, K. Y. Chae, W. R. Hix, M. S. Johnson, K. L. Jones, R. L. Kozub, J. F. Liang, E. J. Lingerfelt, J. Livesay, S. D. Pain, J. P. Scott, M. S. Smith, J. S. Thomas, and D. W. Visser, Physical Review C 10.1103/physrevc.74.045804 (2006).
- [7] A. Matic, A. M. van den Berg, M. N. Harakeh, H. J. Wörtche, G. P. A. Berg, M. Couder, J. Görres, P. LeBlanc, S. O'Brien, M. Wiescher, K. Fujita, K. Hatanaka, Y. Sakemi, Y. Shimizu, Y. Tameshige, A. Tamii, M. Yosoi, T. Adachi, Y. Fujita, Y. Shimbara, H. Fujita, T. Wakasa, B. A. Brown, and H. Schatz, Phys. Rev. C 82, 025807 (2010).
- [8] Y. Parpottas, S. M. Grimes, S. Al-Quraishi, C. R. Brune, T. N. Massey, J. E. Oldendick, A. Salas, and R. T. Wheeler, Phys. Rev. C 70, 065805 (2004).
- [9] J. Caggiano, W. Bradfield-Smith, R. Lewis, P. Parker, D. Visser, J. Greene, K. Rehm, D. Bardayan, and A. Champagne, Physical Review C 65, 055801 (2002).
- [10] N. De Sereville, M. Assié, I. Bahrini, D. Beaumel, M. Chabot, M. Ferraton, S. Fortier, S. Franchoo, S. Giron, F. Hammache, et al., in 11th Symposium on Nuclei in the Cosmos, NIC XI (2010) p. 212.
- [11] J. F. Perello, S. Almaraz-Calderon, B. W. Asher, L. T. Baby, C. Benetti, K. W. Kemper, E. Lopez-Saavedra, G. W. McCann, A. B. Morelock, V. Tripathi, I. Wiedenhöver, and B. Sudarsan, Phys. Rev. C 105, 035805 (2022).
- [12] K. A. Chipps, Phys. Rev. C 93, 035801 (2016).
- [13] M. Basunia and A. Hurst, Nucl. data sheets 134, 1 (2016).
- [14] C. B. Hamill, P. J. Woods, D. Kahl, R. Longland, J. P. Greene, C. Marshall, F. Portillo, and K. Setoodehnia, European Physical Journal. A 56, 10.1140/epja/s10050-020-00052-9 (2020).
- [15] M. Burlein, K. S. Dhuga, and H. T. Fortune, Phys. Rev. C 29, 2013 (1984).
- [16] H. Arciszewski, E. Bakkum, C. Van Engelen, P. Endt, and R. Kamermans, Nuclear Physics A 430, 234 (1984).
- [17] I. Wiedenhöver, L. T. Baby, D. Santiago-Gonzalez, A. Rojas, J. C. BlACKMON, G. V. Rogachev, J. Belarge,

- E. Koshchiy, A. N. Kuchera, L. E. Linhardt, J. Lail, K. T. Macon, M. Matos, and B. C. Rascol, in *Fission and Properties of Neutron-Rich Nuclei* (WORLD SCIENTIFIC, Sanibel Island, Florida, USA, 2013) pp. 144–151.
- [18] P. N. Peplowski, L. T. Baby, I. Wiedenhöver, S. E. Dekat, E. Diffenderfer, D. L. Gay, O. Grubor-Urosevic, P. Höflich, R. A. Kaye, N. Keeley, A. Rojas, and A. Volya, Phys. Rev. C 79, 032801 (2009).
- [19] M. B. Bennett, C. Wrede, K. A. Chipps, J. José, S. N. Liddick, M. Santia, A. Bowe, A. A. Chen, N. Cooper, D. Irvine, E. McNeice, F. Montes, F. Naqvi, R. Ortez, S. D. Pain, J. Pereira, C. Prokop, J. Quaglia, S. J. Quinn, S. B. Schwartz, S. Shanab, A. Simon, A. Spyrou, and E. Thiagalingam, Phys. Rev. Lett. 111, 232503 (2013).
- [20] P. Liang, L. Sun, J. Lee, S. Hou, X. Xu, C. Lin, C. Yuan, J. He, Z. Li, J. Wang, et al., Physical Review C 101, 024305 (2020).
- [21] J. Lai, L. Afanasieva, J. Blackmon, C. Deibel, H. Gardiner, A. Lauer, L. Linhardt, K. Macon, B. Rasco, C. Williams, D. Santiago-Gonzalez, S. Kuvin, S. Almaraz-Calderon, L. Baby, J. Baker, J. Belarge, I. Wiedenhöver, E. Need, M. Avila, B. Back, B. DiGiovine, and C. Hoffman, Nuclear Instruments and Methods in Physics Research Section A: Accelerators, Spectrometers, Detectors and Associated Equipment 890, 119 (2018).
- [22] A. Prochazka, catima, https://github.com/hrosiak/ catima (2021).
- [23] M. Wang, W. Huang, F. Kondev, G. Audi, and S. Naimi, Chinese Physics C 45, 030003 (2021).
- [24] J. Belarge, S. A. Kuvin, L. T. Baby, J. Baker, I. Wiedenhöver, P. Höflich, A. Volya, J. C. Blackmon, C. M. Deibel, H. E. Gardiner, J. Lai, L. E. Linhardt, K. T. Macon, E. Need, B. C. Rasco, N. Quails, K. Colbert, D. L. Gay, and N. Keeley, Phys. Rev. Lett. 117, 182701 (2016).
- [25] L. Canete, G. Lotay, G. Christian, D. Doherty, W. Catford, S. Hallam, D. Seweryniak, H. Albers, S. Almaraz-Calderon, E. Bennett, et al., Physical Review C 104 (2021).
- [26] I. J. Thompson, Computer Physics Reports 7, 167 (1988).
- [27] H. An and C. Cai, Physical Review C 73, 054605 (2006).
- [28] A. Koning and J. Delaroche, Nuclear Physics A 713, 231 (2003).
- [29] W. Richter, B. A. Brown, A. Signoracci, and M. Wiescher, Physical Review C 83, 065803 (2011).
- [30] D. Pérez-Loureiro, C. Wrede, M. B. Bennett, S. N. Liddick, A. Bowe, B. A. Brown, A. A. Chen, K. A. Chipps, N. Cooper, D. Irvine, E. McNeice, F. Montes, F. Naqvi, R. Ortez, S. D. Pain, J. Pereira, C. J. Prokop, J. Quaglia, S. J. Quinn, J. Sakstrup, M. Santia, S. B. Schwartz, S. Shanab, A. Simon, A. Spyrou, and E. Thiagalingam, Phys. Rev. C 93, 064320 (2016).
- [31] L. Janiak, N. Sokołowska, A. A. Bezbakh, A. A. Ciemny, H. Czyrkowski, R. Dąbrowski, W. Dominik, A. S.

Fomichev, M. S. Golovkov, A. V. Gorshkov, Z. Janas, G. Kamiński, A. G. Knyazev, S. A. Krupko, M. Kuich, C. Mazzocchi, M. Mentel, M. Pfützner, P. Pluciński, M. Pomorski, R. S. Slepniev, and B. Zalewski, Phys. Rev. C **95**, 034315 (2017).

- [32] J.-C. Thomas, L. Achouri, J. Äystö, R. Béraud, B. Blank, G. Canchel, S. Czajkowski, P. Dendooven, A. Ensallem, J. Giovinazzo, et al., The European Physical Journal A-Hadrons and Nuclei 21, 419 (2004).
- [33] R. H. Cyburt, A. M. Amthor, R. Ferguson, Z. Meisel, K. Smith, S. Warren, A. Heger, R. Hoffman, T. Rauscher, A. Sakharuk, et al., The Astrophysical Journal Supplement Series 189, 240 (2010).